J. Mod. Transport. (2014) 22(2):65–75
DOI 10.1007/s40534-014-0044-0

www.springer.com/40534

Analysis of steering performance of differential coupling wheelset

Xingwen Wu · Maoru Chi · Jing Zeng · Weihua Zhang · Minhao Zhu

Received: 13 September 2013 / Revised: 12 March 2014 / Accepted: 14 March 2014 / Published online: 19 April 2014

Abstract In order to improve the curving performance of the conventional wheelset in sharp curves and resolve the steering ability problem of the independently rotating wheel in large radius curves and tangent lines, a differential coupling wheelset (DCW) was developed in this work. The DCW was composed of two independently rotating wheels (IRWs) coupled by a clutch-type limited slip differential. The differential contains a static pre-stress clutch, which could lock both sides of IRWs of the DCW to ensure a good steering performance in curves with large radius and tangent track. In contrast, the clutch could unlock the two IRWs of the DCW in a sharp curve to endue it with the characteristic of an IRW, so that the vehicles can go through the tight curve smoothly. To study the dynamic performance of the DCW, a multi-body dynamic model of single bogie with DCWs was established. The self-centering capability, hunting stability, and self-steering performance on a curved track were analyzed and then compared with those of the conventional wheelset and IRW. Finally, the effect of coupling parameters of the DCW on the dynamic performance was investigated.

Keywords Differential coupling wheelset · Independently rotating wheel · Conventional wheelset · Steering performance

1 Introduction

With the development of urban railway transportation, the metro and lower floor light rail vehicles have been widely used in many cities. Whereas, compared with the main line railway vehicles, the urban railway vehicles meet more challenges because of the limitation of circumstance [1–3], which means that the urban railway vehicles may encounter a large number of curved tracks in daily operations, especially tight curves. Therefore, urban railway vehicles require a good steering capability to negotiate the curve with small radius. However, according to the previous operation experience of urban railway vehicles, the conventional wheelset cannot provide sufficient self-steering capability to negotiate the sharp curve, which may leads to severe wheel/rail wear and noise [2–4].

It is well known that the self-steering capability of conventional wheelset mainly depends on the longitudinal creep forces of wheel and rail [1–9]. When the wheelset deviates from the central position of track, the longitudinal creep forces are generated at the wheel/rail contact point due to the conical profile of the wheel tread. With the help of longitudinal creep forces and gravitational restoring forces, the wheelset has the ability to steer itself and return to the central position of track. Thus, the longitudinal creep forces make the conventional wheelset have the self-steering capability in the tangent track and curves [6–8]. To the author's knowledge, conventional wheelsets have enough steering capability in tangent lines and curves with large radii. However, they cannot provide enough steering capability to pass through sharp curves smoothly. The reason is that the difference of rolling radius at the contact point is insufficient to compensate the longer path the outer wheel needs; therefore, the outer wheel begins to skid and continuously contact with flange [5, 8]. In addition, the longitudinal creep forces are also the cause of hunting motion for the conventional wheelset. Once the forward speed of the vehicle exceeds the critical speed, the vehicle

X. Wu (✉) · M. Chi · J. Zeng · W. Zhang · M. Zhu
State Key Laboratory of Traction Power, Southwest Jiaotong University, Chengdu, China
e-mail: xingwen_wu@163.com

would experience the hunting motion, extremely threatening the running safety of vehicles.

In order to resolve the problems of conventional wheelset, many efforts have been made. For example, the semi-active and active actuation systems have been adopted to enhance the dynamic performance of railway vehicles [10, 11]. The independently rotating wheel (IRW) that decouples the wheelset is proposed to eliminate the hunting motion of the conventional wheelset and reduce the wheel/rail wear in sharp curves. The IRWs for railway vehicles have been investigated for many years. However, the use of IRW would also eliminate the guidance capability of the railway vehicles in large radius curves and tangent lines. Consequently, a compromise should be achieved between the curving performance in sharp curves and that in large radius curves and tangent lines by use of active controls like yaw control, creep control of damping, and stiff control. IRWs with profiled tread, with partial coupling, and with a superimposition gearbox have been proposed by Kaplan et al. [12], Dukkipati [13], and Jaschinski et al. [14], respectively. Gretashel and Bose [15] investigated the separate drive motors with precise torque control to provide guidance and curving capability. Goodall and coworkers [16–18] studied the active steering and optimized control strategy for IRWs.

This paper presents a differential coupling wheelset (DCW) to solve the problems of poor curving performance for the conventional wheelset in the sharp curve and bad steering capability for the IRW in the large radius curve and tangent line. In the DCW, both sides of IRWs are coupled by a clutch-type limited slip differential. In the tangent track, the clutch locks the differential, which does not permit a difference in rotation motion of the two wheels, and thus the DCW's dynamic behavior is similar to that of a traditional wheelset. In curves with small radius, the clutch will unlock the differential, and the DCW's dynamic performance is similar to that of a IRW; which can dramatically eliminate the sliding friction between wheel and rail, and reduce the wheel/rail wear and noise in sharp curves. Furthermore, due to the differential, the total rotation speed of two wheels keeps constant. Once the rotation speed of one wheel increases, another wheel decreases at the same time. This difference of rotation speed between two wheels generates a yaw motion for the DCW to negotiate the curves in the radial position to improve the curving performance of urban railway vehicles.

2 Differential coupling wheelset

To investigate the DCW's dynamic performance, two types of DCWs are discussed in this paper: one for a trailer bogie (Fig. 1) and another for a motor bogie (Fig. 2). It can be seen that the DCW consists of two wheels, a solid axle, a hollow axle, and a clutch-type limited slip differential. One wheel is mounted on the left side of a solid axle rigidly, and another wheel is connected to the right side of the solid axle through a bearing. Consequently, two wheels can rotate independently, which means that the DCW has the characteristics of IRWs. However, the guidance capability of an IRW only depends on the gravitational restoring force, which cannot provide enough steering capability. Thus, the clutch-type limited slip differential is used to couple the two IRWs to improve the steering capability of the bogie in large radius curves and tangent lines. The differential has two output gears: one is fixed on the solid axle, and another is connected to the IRW's web through a hollow axle. Since the differential is equipped with a clutch-type limited slip device, it applies a clutch torque to resist the relative motion between the output shafts.

In the multi-body dynamic model, the clutch-type limited slip device is modeled as a torque element combining a spring-damper element with a friction element as shown in Fig. 3. In Fig. 3, K and d, respectively, represent the coupling spring stiffness and coupling damping of the clutch-type limited slip device; $M_{\text{stick(max)}}$ and M_{slip} denote the maximum adhesion torque and the friction torque in the case of slipping.

The characteristics of the DCW can be described as follows:

$$\text{Differential coupling wheelset} = \begin{cases} \text{Traditional wheelset} & M_{\text{w}} < M_{\text{stick(max)}}, \\ \text{Independently rotating wheel} & M_{\text{w}} \geq M_{\text{stick(max)}}, \end{cases}$$

where M_{w} denotes the torque differences of two wheels. When M_{w} exceeds the $M_{\text{stick(max)}}$, the DCW expresses features of an IRW. In contrast, when M_{w} is less than $M_{\text{stick(max)}}$, the DCW has characteristics of a traditional wheelset.

In order to compare the steering performance of DCWs with other types of wheelsets, three types of single bogies, i.e., the bogies with the DCW, IRW, and conventional wheelset, are modeled in this paper, and their steering capabilities are compared in terms of wheel/rail lateral force, friction power, position of contact point on the wheel tread, and so on. In addition, the influence of clutch torque on wheelsets is analyzed.

3 Dynamic performance of bogies with DCWs

3.1 Dynamic model of bogies with DCWs

The trailer bogie and motor bogie with DCWs are modeled as shown in Fig. 4. The trailer bogie consists of two DCWs and a bogie frame (Fig. 4a), whereas the motor bogie is

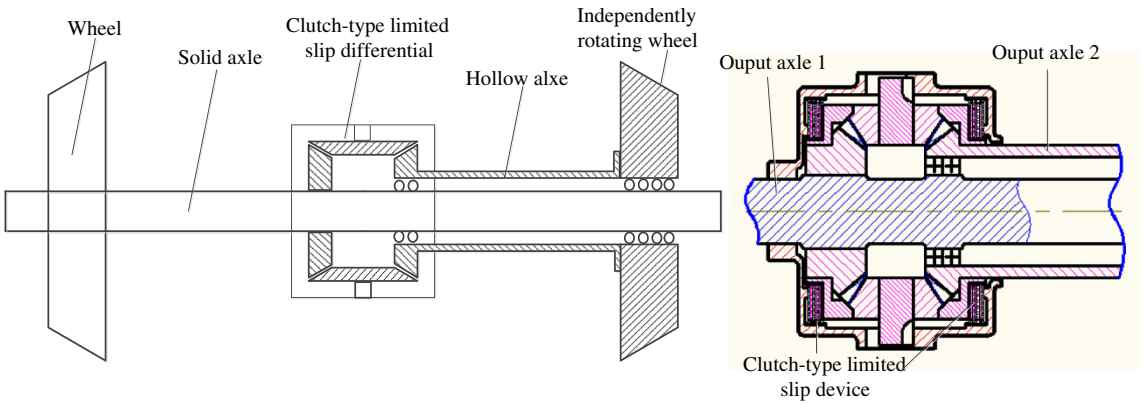

Fig. 1 DCW for trailer bogie

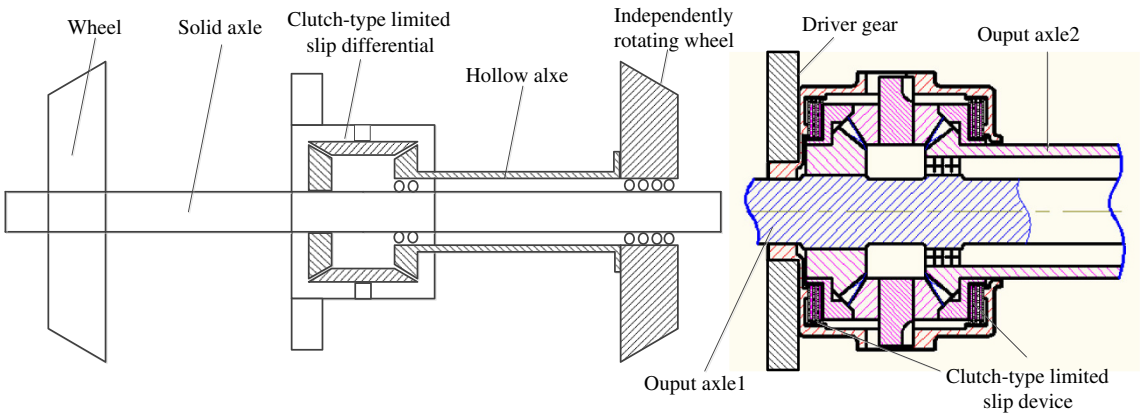

Fig. 2 DCW for motor bogie

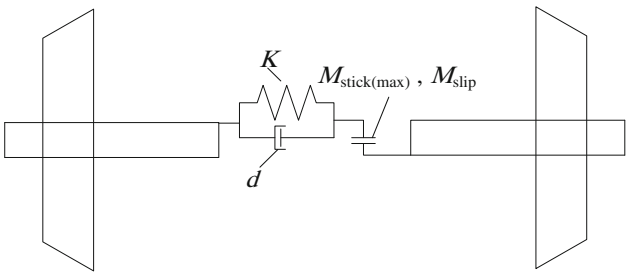

Fig. 3 Torque element of the DCW

composed of two DCWs, two motors, and a bogie frame (Fig. 4b). The DCWs and bogie frame are connected through primary suspensions. We built the dynamic models of the bogies using SIMPACK software. The motors are rigidly fixed on the bogie frame, which has only a pitch motion with respect to the bogie frame. The traction torque is transmitted from motors to the DCW. The gear constraint element is adopted to represent the meshing relationship between the differential and motor. The differential is modeled as a constraint element provided by SIMPACK. The clutch-type limited slip device is represented by a stick–slip rotational torque element. The FSATSIM algorithm is used for the calculation of wheel/rail contact forces. The parameters used in the dynamic models are listed in Table 1, and the degrees of freedom of bogies are shown in Table 2. Figure 5 indicates the wheel/rail contact point and conicity of S1002 wheel tread and 60 rail used in this work.

3.2 Self-centering capability of bogies with DCWs on the tangent line

Self-centering capability is a critical dynamic performance for the wheelset, which indicates the ability of returning to the central position of the track. Figure 6 illustrates a comparative analysis of the lateral displacement for five cases with an initial lateral displacement at the speed of 20 km/h on the tangent line. According to the results, the lateral displacement of the conventional wheelset and the DCW with limited slip device gradually converge to the central position of track. In contrast, the IRW and the DCW without the limited slip device travel to one side of rail from the beginning, and cannot return to the center of track,

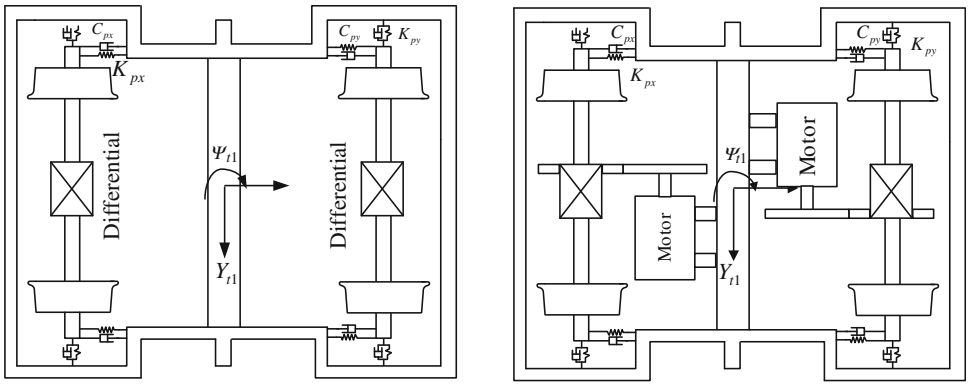

Fig. 4 Bogies with DCWs: **a** Trailer bogie; **b** Motor bogie

Table 1 Parameters used in the model

Bogie mass	3,200 kg
Wheelset mass	1,200 kg
Lateral and longitudinal stiffness of primary suspension	4 MN/m
Vertical stiffness of primary suspension	0.8 MN/m
Radius of wheel	0.325 m
Rail gage	1.435 m
Coefficient of friction	0.4
Coupling stiffness	60 kNm/rad
Coupling damping	60 kNms/rad
Max adhesion torque	500 Nm

which causes continuous flange contact, and severe wheel/rail wear and noise. The comparison analysis results indicate that the limited slip device plays a vital role in the dynamic performance of the DCW. The DCW could express the features of the IRW without the limited slip device. On the contrary, with the help of limited slip device, DCW could have a good self-centering capability of the conventional wheelset.

In order to acquire enough steering capability, the clutch-type limited slip device is applied into the differential for coupling two wheels. Figure 7 indicates the influence of coupling stiffness and damping on the lateral displacement of the DCW. As the coupling stiffness K and damping d increase, the lateral displacement of wheelset gradually converges to the central position of the track. This reflects that the increased coupling stiffness and damping is good for the improvement of steering performance. However, if the coupling stiffness and damping do not match reasonably, the DCW may show a "hunting motion." This motion is not a definite hunting motion but just a quasi-hunting motion, which is mainly induced by the self-excited oscillation of coupling stiffness and damping. Therefore, it is necessary to optimize the coupling parameters to ensure a good guidance capability of the DCW.

3.3 Stability analysis of the bogie with DCW

Once the operation speed of a vehicle exceeds the critical speed, the vehicle gives rise to a hunting motion in the lateral direction, which extremely threatens the operation safety of the vehicle. Therefore, the critical speed of vehicles should be larger than the maximum operation speed. Since low coupling stiffness and coupling damping cause the self-excited oscillation as shown in Fig. 7, the coupling stiffness K and coupling damping d are set to 100 kNm/rad and 100 kNms/rad, respectively, for stability analysis of the bogie. Figure 8 illustrates the bifurcation diagram of the bogie with DCW. It can be seen that the

Table 2 Degrees of freedom

Vehicle model	Type of motion					
	Longitudinal	Lateral	Vertical	Roll	Yaw	Pitch
Bogie frame	V	V	V	V	V	V
Differential coupling wheelset	V	V	V	V	V	V
Axle box	–	–	–	–	–	V
Motor	–	–	–	–	–	V

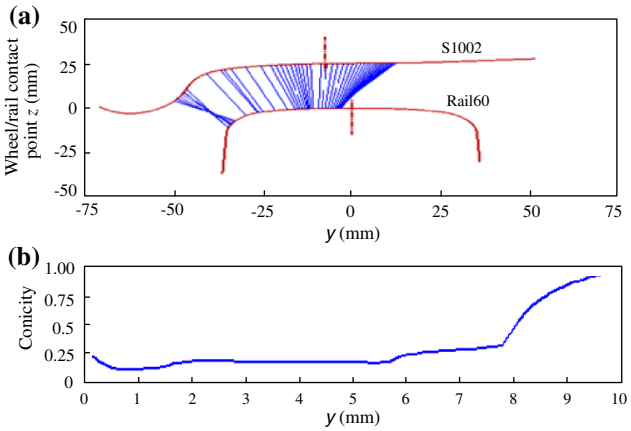

Fig. 5 Wheel/rail contact point (**a**); conicity (**b**) of S1002 and Rail 60

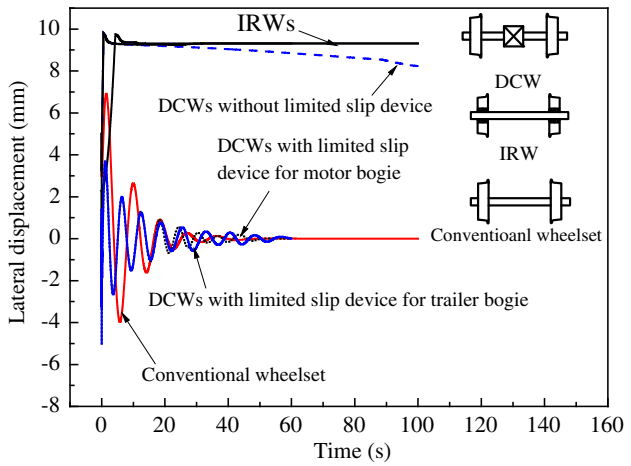

Fig. 6 Lateral displacement of wheelset

type of bifurcation is a typical supercritical Hopf bifurcation. In Fig. 8, point A represents the linear critical speed of bogie, and $V_A = 115$ km/h; point B denotes the nonlinear critical speed of bogie, and $V_B = 85$ km/h; the dash line indicates the unstable limited cycle; and the solid line indicates the stable limited cycle. When the vehicle speed V is less than V_B, the motion of the vehicle is always stable. When the vehicle speed is between V_B and V_A, the motion of the vehicle largely depends on the initial conditions. Figure 9 indicates the influence of coupling stiffness and coupling damping on the critical speed of the bogie with DCW. With increasing the coupling damping, the critical speed of the bogie increases sharply when the coupling damping is less than 50 kNms/rad. However, when the coupling damping exceeds 50 kNms/rad, the critical speed tends to be stable. In addition, the coupling stiffness has little influence on the critical speed.

3.4 Self-steering ability of the trailer bogie with DCW

To analyze the self-steering ability of the DCW, the curving performances of three types of bogies are compared in terms of wheel/rail lateral force, friction power, and position of contact point on the wheel tread. Figure 10 indicates the layout of curved track. The parameters of simulation track are listed in Table 3.

Generally, the bogie is guided in the curve section primarily by the lateral forces on the front wheelset. Thereby the lateral forces on the front wheelsets of the three types of bogies are analyzed, as shown in Fig. 11. It can be seen that the lateral forces on the outer IRW are smaller than the other two types of wheelsets. The reason is that the bogie with the conventional wheelset or DCW cannot adjust radially to full extent while the IRW can adapt better to the radial position of the curved track. Compared with the conventional wheelset, the DCW is much easier to negotiate the curve in radius position with the help of clutch-

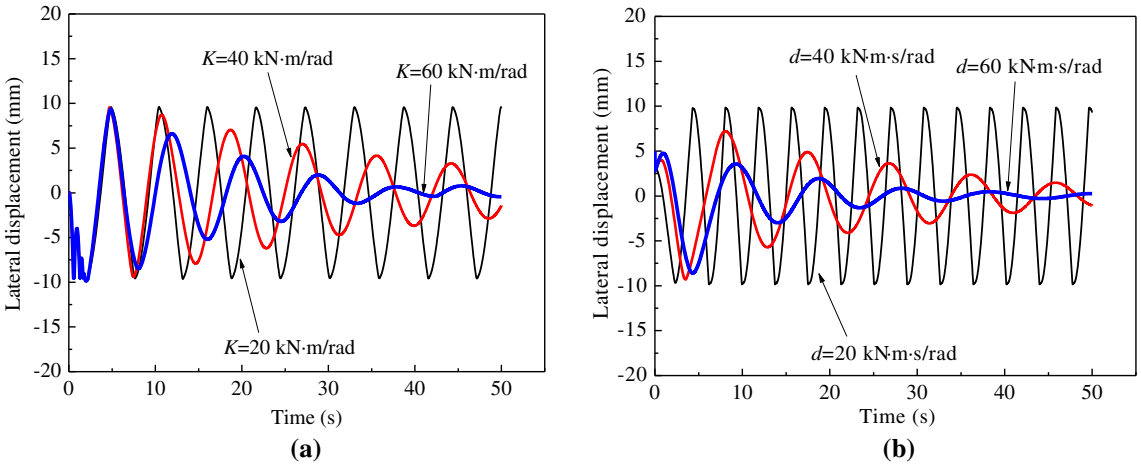

Fig. 7 Influence of coupling parameters on the lateral displacement of the DCW for different coupling stiffness K (**a**); different coupling damping d (**b**)

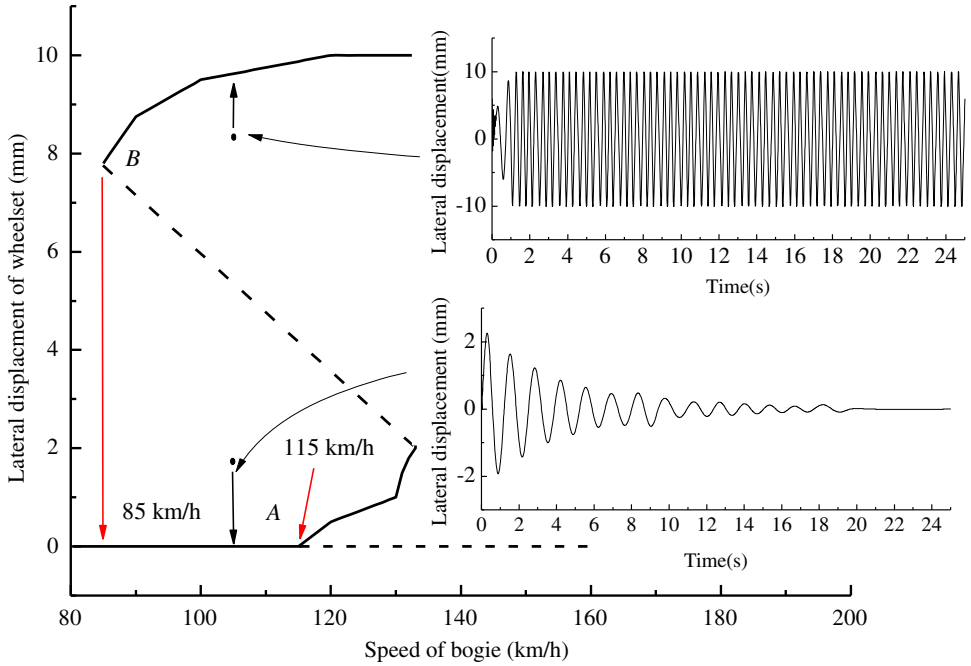

Fig. 8 Bifurcation diagram of the bogie with DCW

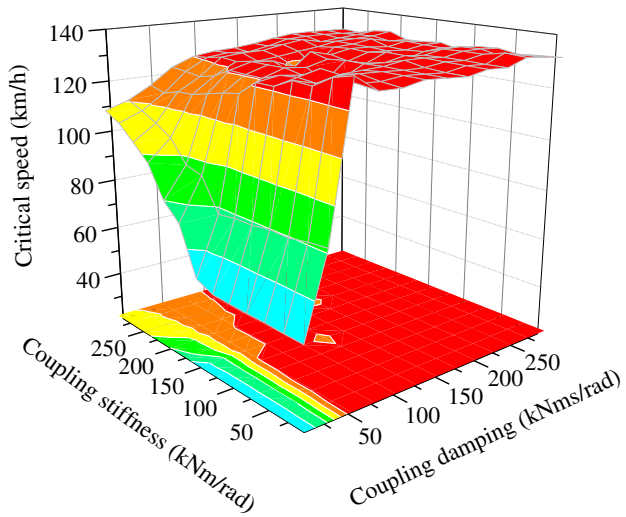

Fig. 9 Influences of coupling stiffness and coupling damping on the critical speed

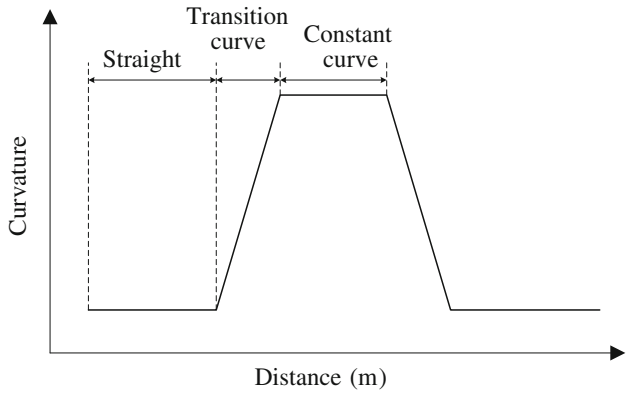

Fig. 10 Layout of simulation track

Table 3 Parameters of simulation track

Length of tangent track (m)	150
Length of transition track (m)	20
Length of constant curve (m)	50
Radius of curve (m)	30
Cant (m)	0
Running speed (km/h)	20

type limited slip differential, which could convert the slip friction to the rolling friction to reduce wheel/rail wear and noise, and generates small lateral forces and friction power to the solid wheelsets.

In addition, the frictional power as a wear index is investigated, and the result is shown in Fig. 12. The frictional power is calculated by the creep forces and the corresponding creep velocities within the local contact coordinate system. Compared with the conventional wheelset, the DCW has a better wear index because of its IRW characteristics.

Figure 13 shows the position of contact points on the wheel tread. The lateral displacement of contact points on the wheel of DCW is apparently smaller than that on the traditional wheelset. Furthermore, after the DCW goes through the curve section, the wheelset gradually returns to the central position of track. However, the IRW goes to one

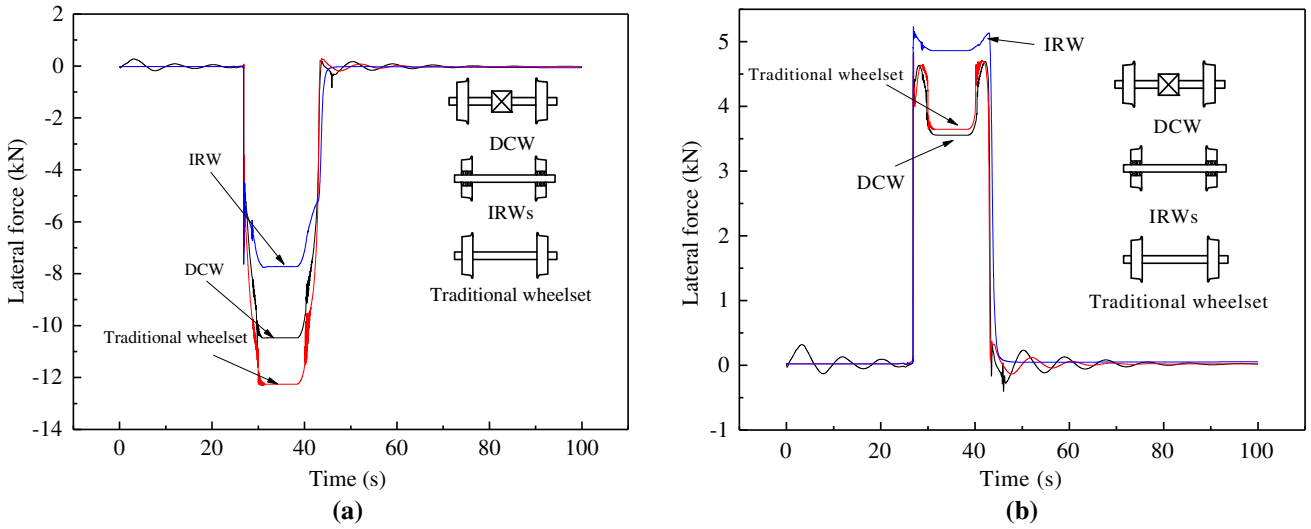

Fig. 11 Wheel/rail lateral forces: **a** Outer wheel; **b** Inner wheel

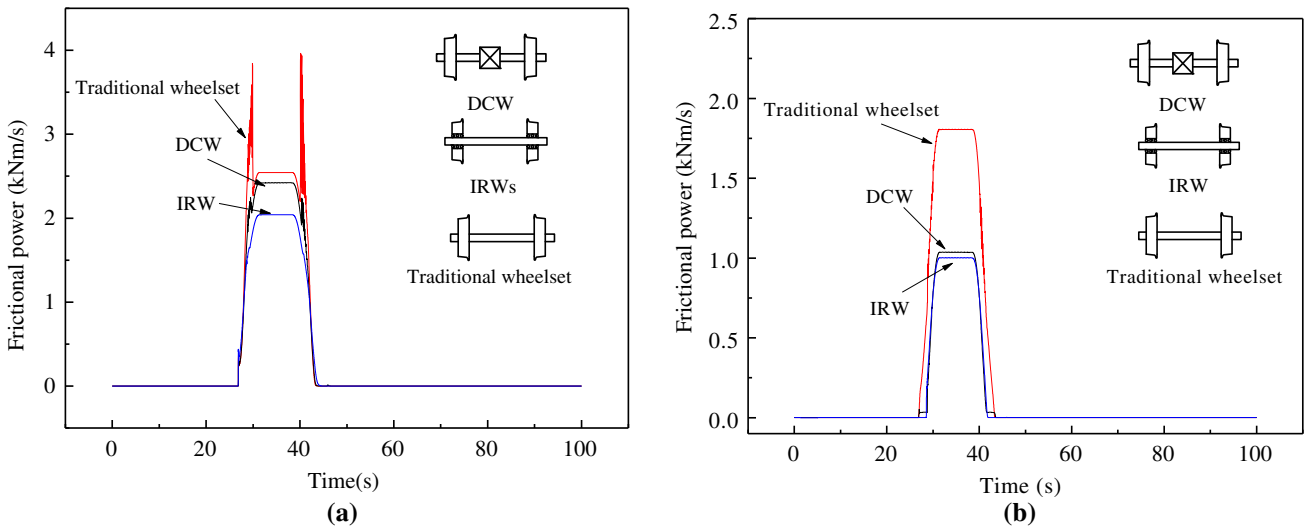

Fig. 12 Friction power: **a** Front wheelset; **b** Rear wheelset

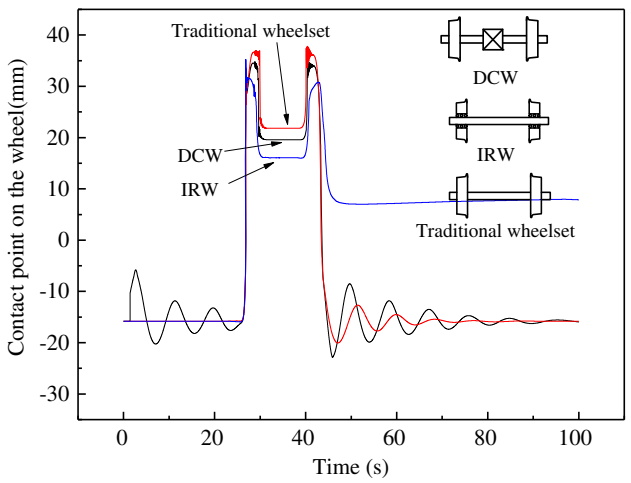

Fig. 13 Lateral displacement of contact points

side of rail and cannot return to the central position of track, resulting in eccentric wear of wheel and rail.

Figure 14 illustrates the rotation speed difference that occurs in the curve section due to the differential. As the rotation speed of the outer wheel increases, the inner wheel decreases. This endues the DCW with good self-steering performance and curving performance. When the wheelset gets out from the curve section, the clutch-type limited slip device locks the wheels at both sides so that the two wheels have the same rotation speed. In contrast, the IRW cannot return to the center of track, which makes the speeds of two wheels different.

From the above comparison, we can come to a conclusion that the DCW has better curving performance than the conventional wheelset. Due to the torque of the clutch-type limited slip device, the DCW can also express better self-

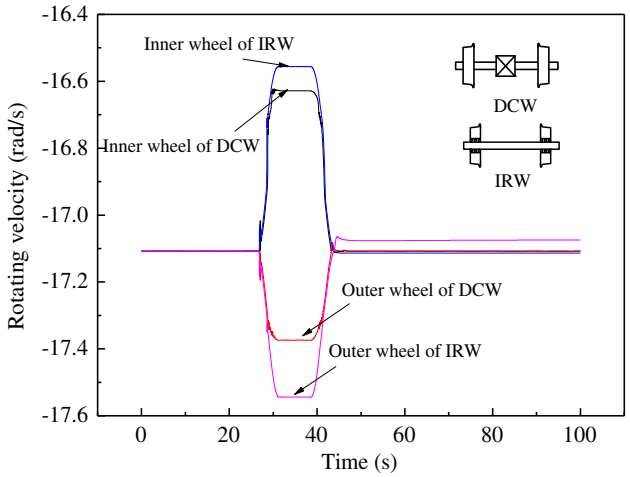

Fig. 14 Rotation speed of differential wheelsets

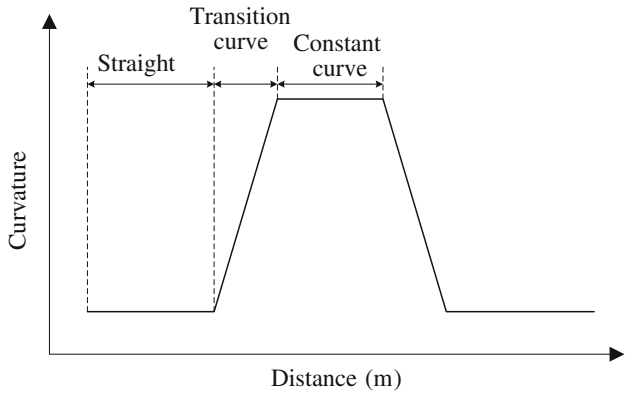

Fig. 15 Layout of simulation track

Table 4 Parameters of simulation track

Length of tangent track (m)	100
Length of transition track (m)	20
Length of constant curve (m)	50
Radius of curve (m)	50
Cant (m)	0

steering performance than the IRW. Therefore, the DCW processes the good curving performance of an IRW and the self-steering capability of the conventional wheelset.

3.5 Self-steering ability of motor bogie with the DCW

When the DCW is applied to a motor bogie, the differential is used to transmit the traction torque. It also allows both the wheels to rotate at different speeds, which differentiates it from the conventional wheelset. In the following, single motor bogies with DCW and traditional wheelset are analyzed and compared when the bogie goes through a curved track at a constant speed with the action of traction motor. The curved track is shown in Fig. 15, and the parameters are listed in Table 4.

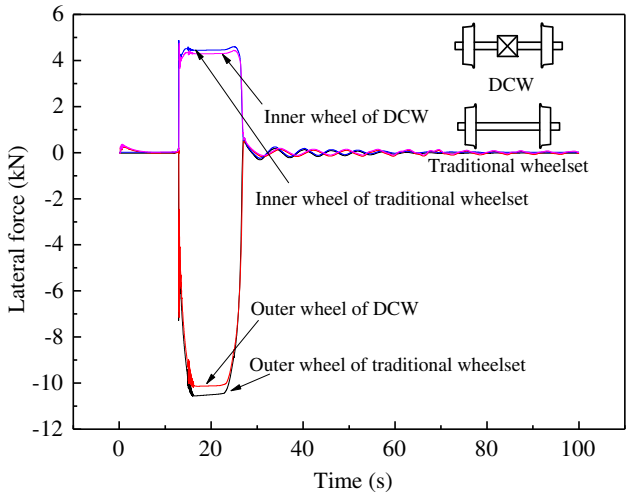

Fig. 16 Wheel/rail lateral force

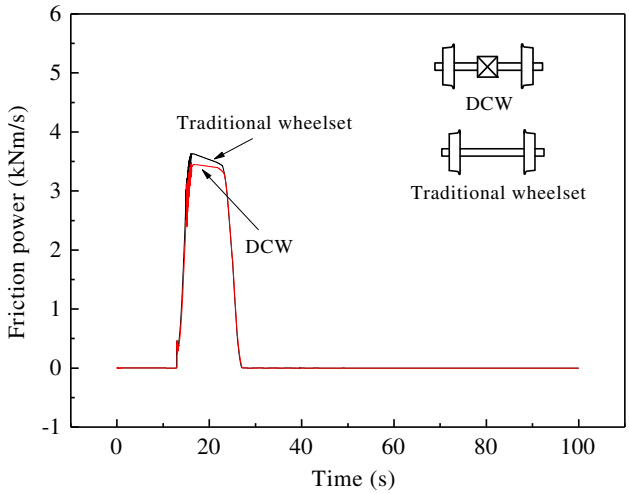

Fig. 17 Friction power

Figures 16 and 17 indicate the wheel/rail lateral force and friction power of the front wheelset for the two types of bogies. As can be seen from Fig. 16, the wheel/rail lateral force of the DCW is apparently smaller than that of the traditional wheelset in the curve section. Furthermore, comparison of the friction power of the two kinds of wheelset in Fig. 17 indicates that the DCW is superior to the traditional wheelset in the curving performance. Therefore, a conclusion can be drawn that in the case of motor bogie, the DCW has a better self-steering capability than the traditional wheelset.

3.6 Influence of coupling parameters on the DCW's dynamic performance

The clutch torque of the clutch-type limited slip device has a critical effect on the dynamic behavior of the DCW, and

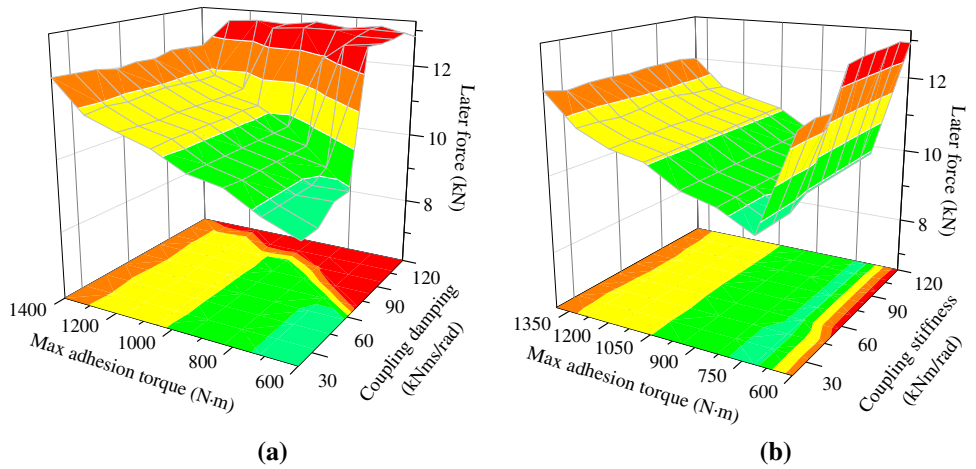

Fig. 18 Influence of coupling parameters on the lateral force of DCW: **a** Maximum adhesion torque $M_{\text{stick(max)}}$ versus coupling damping with coupling stiffness $K = 60$ kNm/rad; **b** Maximum adhesion torque $M_{\text{stick(max)}}$ versus coupling stiffness with coupling damping $d = 60$ kNms/rad

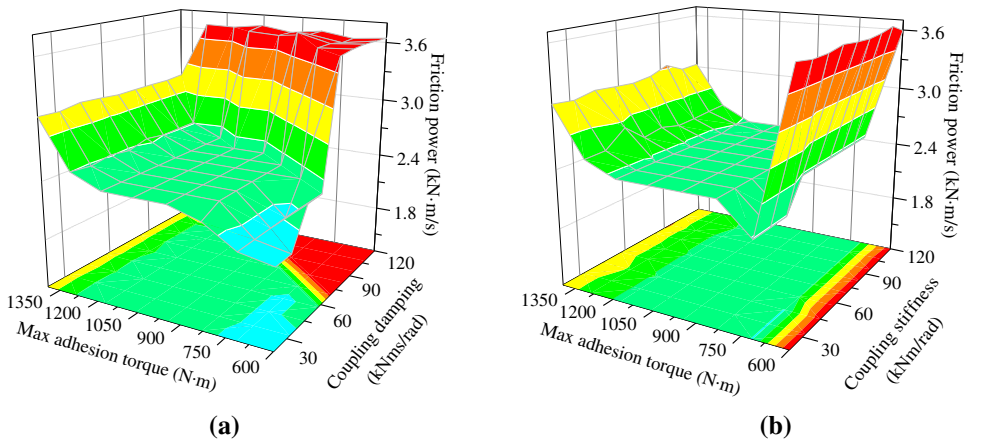

Fig. 19 Influence of coupling parameters on the friction power of DCW: **a** Maximum adhesion torque $M_{\text{stick(max)}}$ versus coupling damping with coupling stiffness $K = 60$ kNm/rad; **b** Maximum adhesion torque $M_{\text{stick(max)}}$ versus coupling stiffness with coupling damping $d = 60$ kNms/rad

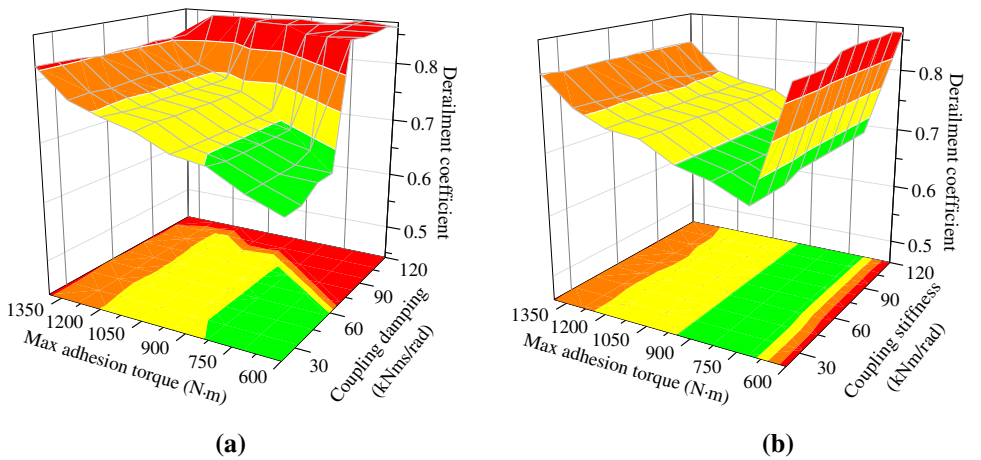

Fig. 20 Influence of coupling parameter on the derailment coefficient of DCW: **a** Maximum adhesion torque $M_{\text{stick(max)}}$ versus coupling damping with coupling stiffness $K = 60$ kNm/rad; **b** Maximum adhesion torque $M_{\text{stick(max)}}$ versus coupling stiffness with coupling damping $d = 60$ kNms/rad

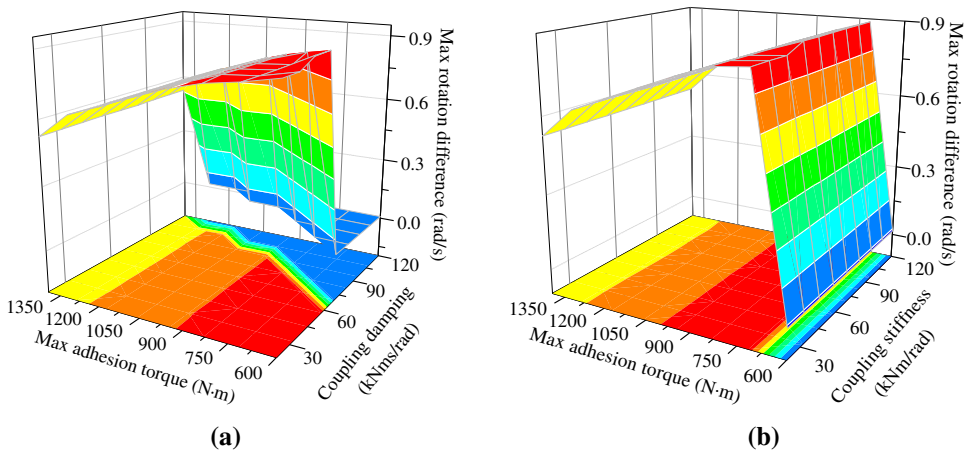

Fig. 21 Influence of coupling parameter on the maximum rotation difference of DCW: **a** Maximum adhesion torque $M_{\text{stick(max)}}$ versus Coupling damping with coupling stiffness $K = 60$ kNm/rad; **b** Maximum adhesion torque $M_{\text{stick(max)}}$ versus Coupling stiffness with coupling damping $d = 60$ kNms/rad

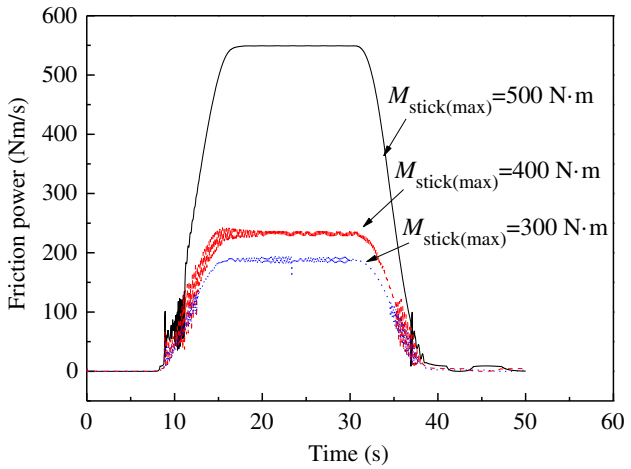

Fig. 22 Friction power

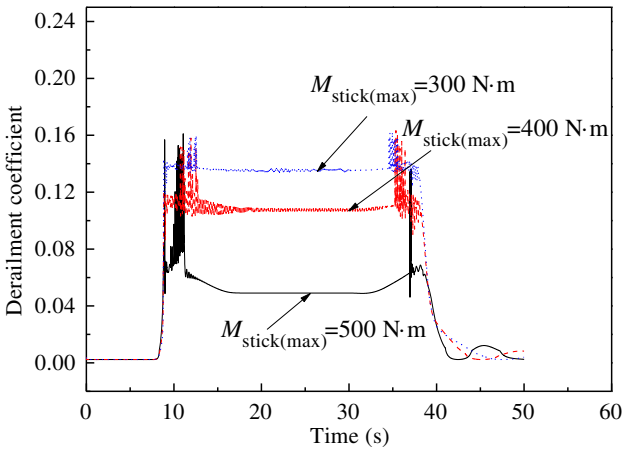

Fig. 23 Derailment coefficient

determines the work conditions of the differential. Therefore, the influence of the maximum adhesion torque and other coupling parameters of the clutch-type limited slip differential on the curving performance are investigated in this section.

Figure 18 illustrates the influence of the maximum adhesion torque, coupling stiffness, and coupling damping on the lateral wheel/rail force. With increasing the maximum adhesion torque and coupling damping, the lateral forces of wheel/rail increase (Fig. 18a). Compared with the coupling damping, however, the influence of the coupling stiffness is smaller (Fig. 18b). Due to the increased maximum adhesion torque, the torque difference between two wheels is more difficult to exceed the maximum adhesion torque, which causes that both wheels cannot rotate independently, and thus express more features of the conventional wheelset. As shown in Figs. 19 and 20, with increasing the maximum adhesion and coupling damping, the friction power and derailment coefficient increase. Meanwhile, the coupling damping dramatically reduces the relative speed of the two wheels, as shown in Fig. 21. According to the simulation results, the coupling stiffness has little influence on the dynamic performance of the DCW.

4 Discussions

As mentioned above, small maximum adhesion torque and small coupling damping are beneficial to improving the DCW's curving performance, which endue the DCW with properties of IRWs. However, too small maximum adhesion torque and coupling damping could deteriorate the DCW's self-steering performance in large radius curves and tangent lines. Generally, the maximum adhesion torque determines the work conditions of the DCW, and it

depends on the wheel/rail adhesion conditions affected by many factors [19–22], such as normal load, sliding speed, temperature of the two bodies, contact geometry, weather conditions, and the presence of rain, snow, and dead leaves. On the other hand, with the reduction of the maximum adhesion torque, the friction power decreases (Fig. 22) and the derailment coefficient increases (Fig. 23). Therefore, a compromise should be achieved between running safety and wheel/rail wear.

5 Conclusions and future work

According to the simulation results, the DCW integrates both the features of the IRW and the conventional wheelset. In tight curves, the DCW can express the features of IRWs to achieve an improvement in the curving performance over the conventional wheelset. In tangent lines and large radius curves, the DCW has a self-steering capability as the conventional wheelset.

The study of coupling parameters shows that the maximum adhesion torque and coupling damping have a large influence on the dynamic behavior of DCW. With the increasing of the maximum adhesion torque and the coupling damping, the DCW tends to be a conventional wheelset. The maximum adhesion torque of the clutch-type limited slip device depends on the wheel/rail adhesion conditions.

However, in this paper we have only discussed the dynamic performance of single bogies, through which the maximum adhesion torque could not be determined and hence we cannot investigate how to control the maximum adhesion torque to adapt to different track conditions. Therefore, in the future research, the creep control will be studied to determine the maximum adhesion torque of clutch-type limited slip device with the full railway vehicle.

Acknowledgments This work was supported by the National Key Technology R&D Program of China (No. 2009BAG12A02), the National Basic Research Program of China (No. 2011CB711106), the Program for Innovative Research Team in University (No. IRT1178), the Program for New Century Excellent Talents in University (No. NCET-10-0664), and the National Key Technology R&D Program (No. 2009BAG12A01).

References

1. Kuba T, Lugner P (2012) Dynamic behaviour of tramways with different kinds of bogies. Veh Syst Dyn 50(S1):277–289
2. Shen G, Zhou J, Ren L (2006) Enhancing the resistance to derailment and side-wear for a tramway vehicle with independently rotating wheels. Veh Syst Dyn 44(S1):641–651
3. Garg VK, Dukkipati RV (1984) Dynamics of railway vehicle system. Academic Press, Toronto, pp 145–165
4. Dukkipati RV (1992) Independently rotating wheel system for railway vehicles: a state of the art review. Veh Syst Dyn 21(1):297–330
5. Ahmed AKW, Sankar S (1987) Lateral stability behavior of railway freight car system with elasto-damper coupled wheelset (part 2): truck model. Transm Autom Des 109(12):500–507
6. Ahmed AKW, Sankar S (1988) Steady-state curving performance of railway freight truck with damper-coupled wheelsets. Veh Syst Dyn 17(6):295–315
7. Chi M, Zhang W, Wang K, Zhang J (2003) Research on dynamic stability of the vehicle with coupled wheelsets. J Tongji Univ 31(4):464–468
8. Chi M, Wang K, Fu M, Ni W, Zhang W (2002) Analysis on wheel-rail lateral force of the bogie with independently rotating wheels for rear wheelsets. J Traffic Transp Eng 2(2):184–192
9. Satou E, Miyamoto M (1992) Dynamic of a bogie with independently rotating wheels. Veh Syst Dyn 20(1):519–534
10. Allotta B, Pugi L, Bartolini F, Cangioli F, Colla V (2010) Comparison of different control approaches aiming at enhancing the comfort of a railway vehicle. In: 2010 IEEE/ASME international conference on advanced intelligent mechatronics (AIM), Montreal, pp 676–681
11. Allotta B, Pugi L, Colla V, Bartolini F, Cangioli F (2011) Design and optimization of a semi-active suspension system for railway applications. J Mod Transp 19(4):223–232
12. Kaplan A, Hasselman TK, Short SA (1970) Independently rotating wheels for high speed trains. SAE Paper 700841
13. Dukkipati RV (1978) Dynamics of independently rotating wheelsets: a survey of the state of the art. Tech. Rep. LTR-IN-398, NRC Railway Laboratory
14. Jaschinski A, Chollet H, Iwnicki S, Wickens A, Von Würzen J (1999) The application of roller rigs to railway vehicle dynamics. Veh Syst Dyn 31(5–6):345–392
15. Gretzschel M, Bose L (2002) A new concept for integrated guidance and drive of railway running gears. In: Proceedings of the 1st IFAC conference on mechatronic systems, vol 1, Darmstalt, pp. 265–270
16. Goodall R, Mei TX (2005) Mechatronic strategies for controlling railway wheelsets with independently rotating wheels. In: Proceedings of the IEEE/ASME international conference on advanced intelligent mechatronicsn (AIM'05), vol 1, Como, Italy, pp. 225–230
17. Mei TX, Goodall RM (2001) Robust control for independently rotating wheelsets on a railway vehicle using practical sensors. IEEE Trans Control Syst Technol 9(4):599–607
18. Mei TX, Goodall RM (2003) Practical strategies for controlling railway wheelsets independently rotating wheels. J Dyn Syst Meas Control Trans ASME 125(3):354–360
19. Powell AJ, Wickens AH (1996) Active guidance of railway vehicles using traction motor torque control. Veh Syst Dyn 25(S1):573–584
20. Wickens AH (2009) Comparative stability of bogie vehicles with passive and active guidance as influenced by friction and traction. Veh Syst Dyn 47(9):1137–1146
21. Conti R, Meli E, Pugi L, Malvezzi M, Bartolini F, Allotta B, Rindi A, Toni P (2012) A numerical model of a HIL scaled roller rig for simulation of wheel–rail degraded adhesion condition. Veh Syst Dyn 50(5):775–804
22. Malvezzi M, Pugi L, Papini S, Rindi A, Toni P (2013) Identification of a wheel–rail adhesion coefficient from experimental data during braking tests. Proc Inst Mech Eng F 227(2):128–139